solved by a fourth-order Runge-Kutta technique with $ij = 2.0$ and $D = 14.7$ which corresponds to nitrogen. The starting values of ψ and ϕ were obtained for a given ξ from the equilibrium solution ($\psi = \phi$) given by Eq. (7). The reference entropy S_r value in Eq. (7) was taken as 15.5. The factors f_1, f_2 and f_3 were all assumed to be zero. The starting values of ξ for different χ values were selected in such a way that the solution always started with equilibrium conditions.

A series of solutions for different values of χ for nitrogen are shown in Fig. 1. The vibrational temperature function ϕ is seen to follow the translational function ψ very closely for awhile, the extent of which depends on χ and then diverges rather suddenly and reaches a constant value, this corresponds to the freezing of the vibrational energy mode. The translational temperature function ψ increases monotonically as ξ decreases. The equilibrium solution shown in Fig 1 is also given by the envelope of all the nonequilibrium solutions.

It has been shown that the nonequilibrium similar solutions depend on two general parameters ξ and χ. In order to use the similar solutions presented in this paper (Fig. 1) the parameters ξ and χ should be known in terms of the initial and boundary values. Therefore, the functional dependence of ξ and χ must be considered. The parameter ξ is a function of not only the reservoir and nozzle throat conditions, but also of velocity. In Ref. 6 it is shown that a modified velocity ratio u'/u_*' can be well correlated with the area ratio A'/A_*'. This leads to a simple expression for a modified velocity ratio which is used in finally expressing ξ as

$$\xi = \psi_0/(e^{\psi_0} - 1) - \log_e\{k_1^{-4}k_2^{-1}\psi_0^{5/2}(1 - e^{-\psi_0}) \times A[0.5 - 0.31(1 + \log_{10}A)^{-2}]\} + S_r \quad (10)$$

(The constants k_1 and k_2 are given in Ref. 6.) It is noted that ξ depends on only two parameters, namely, the area ratio and the reservoir temperature function ψ_0. The parameter ξ is now expressed in terms of the initial and boundary values only and hence can be readily computed for any given conditions.

The parameter χ can be shown[6] to reduce to

$$\chi = \log_e\left[k_1^{(6+1/ij)}\left(\frac{m}{R\theta_v}\right)^{1/2}\left(\frac{p_0'}{C}\right)L\psi_0^{(4-2.5/ij)} \times (1 - e^{-\psi_0})^{(1-1/ij)}\right] - \left(1 - \frac{1}{ij}\right)\left[\frac{\psi_0}{e^{\psi_0} - 1} + S_r\right] \quad (11)$$

It is noted that χ is independent of A. Also, for a given gas χ depends on only p_0', L and ψ_0 since θ_0, C and S_r are all constants.

To apply the results presented here, ξ and χ values can be computed using Eqs. (10) and (11) based on known reservoir conditions and area ratio. Then, using these ξ and χ values, along with Fig. 1, ϕ and ψ values can be determined with which the algebraic governing equations can be used to determine p, ρ and u.

Range of Applicability of the Parameter χ

The general correlating parameter χ depends on p_0', L and ψ_0 for a given gas. The variation of $p_0'L$ with ψ for a constant χ was computed using Eq. (11) and is shown in Fig. 2 for a number of χ values. The variation of $p_0'(L = 1.0)$ with ψ_0 for a constant equilibrium mole fraction of 0.1 is also shown; this curve represents approximately the high temperature limit beyond which dissociation relaxation may have to be considered. A curve is also shown which indicates the maximum ψ value, for a given χ, where the nonequilibrium solution departs from the equilibrium solution. For reservoir conditions defined by the region above this line, the solutions start with equilibrium conditions and can be obtained from the present similar solutions. For reservoir conditions defined by the region well below this line the flow can be considered as frozen in the entire nozzle. In a narrow region just below the equilibrium limit line the flow will be in the nonequilibrium state and the solutions have to be obtained by starting with the reservoir conditions as the initial values.

Conclusions

Based on the present analysis the following conclusions are reached. 1) Similar solutions for vibrational nonequilibrium nozzle problems can be obtained over a wide range of initial conditions and nozzle scale parameters by using the new similarity parameter ξ. 2) The parameters ξ and χ serve as general correlating parameters since they contain all the parameters of the problem. The vibrational equilibrium solutions depend on the one parameter χ only and the nonequilibrium solutions depend on two parameters χ and ξ.

References

[1] Stollery, J. L. and Smith, J. E., "A Note on the Vibration of Vibrational Temperature Along a Nozzle," *Journal of Fluid Mechanics*, Vol. 13, 1962, pp. 225–235.

[2] Stollery, J. L. and Park, C., "Computer Solutions to the Problem of Vibrational Relaxation in Hypersonic Nozzle Flows," *Journal of Fluid Mechanics*, Vol. 19, 1964, pp. 113–123.

[3] Erickson, W. D., "Vibrational-Nonequilibrium-Flow of Nitrogen in Hypersonic Nozzles," TN D-1810, June 1963, NASA.

[4] Hall, J. G. and Treanor, C. E., "Nonequilibrium Effects in Supersonic-Nozzle Flows," Rept. 163, March 1968, Cornell Aeronautical Lab., Buffalo, N.Y.

[5] Anderson, J. D., "A Time-Dependent Analysis for Vibrational and Chemical Nonequilibrium Nozzle Flows," *AIAA Journal*, Vol. 8, No. 3, March 1970, pp. 545–550.

[6] Reddy, N. M. and Daum, F. L., "Similar Solutions in Vibrational Nonequilibrium Nozzle Flows," AIAA Paper 70-804, Los Angeles, Calif., 1970.

Time-Dependent Numerical Analysis of MHD Blunt Body Problem

James F. Coakley* and Robert W. Porter†

Illinois Institute of Technology, Chicago, Ill.

THE interaction of shock heated plasma and an onboard magnet may prove attractive for an atmospheric entry vehicle (Fig. 1). A review of the subject is contained in Ref. 1.

In the present work, the time dependent finite difference method[2] is applied. Results are compared with those of

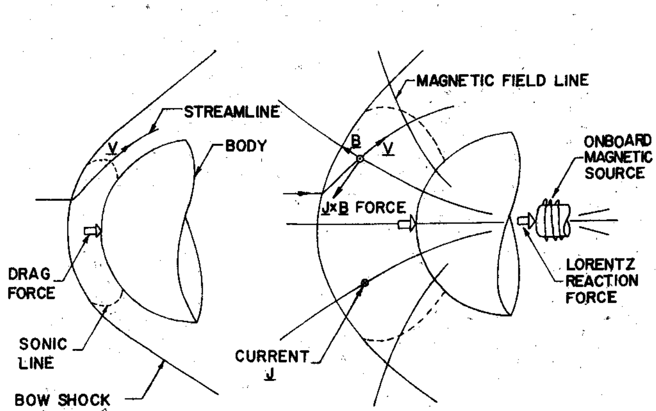

Fig. 1 Effect of onboard magnetic source.

Presented as Paper 70-760 at the AIAA 3rd Fluid and Plasma Dynamics Conference, Los Angeles, Calif., June 29–July 1, 1970; submitted August 7, 1970; revision received March 19, 1971. This work supported by National Science Foundation under GK-2844.

* Research Assistant, Mechanical and Aerospace Engineering Department. Student Member AIAA.

† Assistant Professor, Mechanical and Aerospace Engineering Department. Member AIAA.

more approximate work dealing mainly with the stagnation region[3-7] and with the method of integral relations.[8] Inviscid, ideal gas flow without reactions or radiation is considered. The electrical conductivity is assumed to be a scalor and a power of absolute temperature. The magnetic Reynolds number is vanishingly small. The magnetobody is a hemisphere with an aligned dipole at the origin under conditions of axisymmetry.

An initial valve problem is formulated. The bow shock is treated as a moving discontinuity and is coupled to the adjacent shock layer using multidimensional characteristics. The shock layer is treated using the equations of unsteady motion and the Lax difference method.[9] The system is advanced in time toward the steady state of interest.

The unsteady equations for the shock layer are[2]

$$\partial \rho/\partial t = -\rho\nabla\cdot\mathbf{V} - \mathbf{V}\cdot\nabla\rho \tag{1}$$

$$\partial \mathbf{V}/\partial t = -\mathbf{V}\cdot\nabla\mathbf{V} - (\nabla p - \mathbf{F})/\rho \tag{2}$$

$$\partial s/\partial t = -\mathbf{V}\cdot\nabla s + q/(\rho T) \tag{3}$$

where[8] the body force is $\mathbf{F} = \sigma(\mathbf{V}\times\mathbf{B})\times\mathbf{B}$ and the dissipation is $q = \sigma(\mathbf{V}\times\mathbf{B})\cdot(\mathbf{V}\times\mathbf{B})$ where ρ is density, $\mathbf{V}$ velocity, $p(\rho,s)$ pressure, s specific entropy, $\sigma \propto T^{\omega}$ electrical conductivity, $T(\rho,s)$ absolute temperature and $\mathbf{B}(\mathbf{r})$ is the magnetic dipole field. Spherical coordinates were used in the computation.

The equations for the bow shock include the shock conservation relations and an additional relation which couples the shock to the shock layer. The additional relation[10] is rom the method of characteristics as generalized to MHD dow at vanishing magnetic Reynolds number.[11] A similar approach is employed at the body surface. The objective is to avoid noncentral differences at boundaries which may lead to a pseudo boundary layer.

The region of calculation is closed downstream by a surface in locally supersonic flow extending radially from the hemisphere shoulder to the bow shock. Differences normal to that surface are evaluated by linear extrapolation.

The nondimensional groups involved are the Mach number $M_\infty = V_\infty/a_\infty$ where a is the speed of sound, the specific heat ratio γ, the magnetic interaction parameter $Q = \sigma_0 B_0{}^2 R_0/(\rho_\infty V_\infty)$ where R is the body radius, and the exponent ω on which the conductivity depends on temperature. The subscripts 0 and ∞ denote the stagnation point and the freestream, respectively.

The shock layer is mapped onto a stationary rectangular domain bounded by the shock, axis of symmetry, body and downstream surface by $\varphi = (r - r_b)/(r_s(\theta,t) - r_b)$ and $\Theta = \theta$ where b denotes body and s shock. The nondimensional time is $\tau = a_\infty t/(R_0\gamma^{1/2})$. The system Eqs. (1–3) can be represented by

$$\partial \mathbf{f}/\partial\tau = \mathbf{g}(\varphi,\Theta,\tau) \tag{4}$$

where $\mathbf{g}$ contains derivatives in φ and Θ. Using the Lax difference scheme, the variables are advanced in time

$$\mathbf{f}(\varphi,\Theta,\tau + \Delta\tau) = \bar{\mathbf{f}}(\varphi,\Theta,\tau) + \mathbf{g}(\varphi,\Theta,\tau)\Delta\tau \tag{5}$$

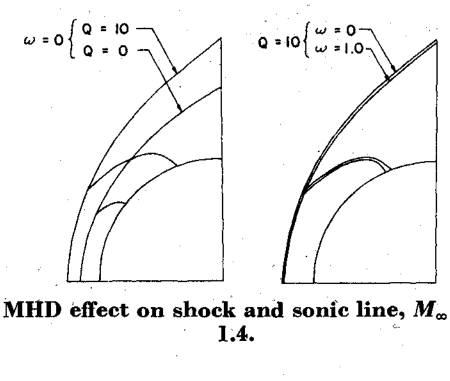

Fig. 2 MHD effect on shock and sonic line, $M_\infty = 5$, $\gamma = 1.4$.

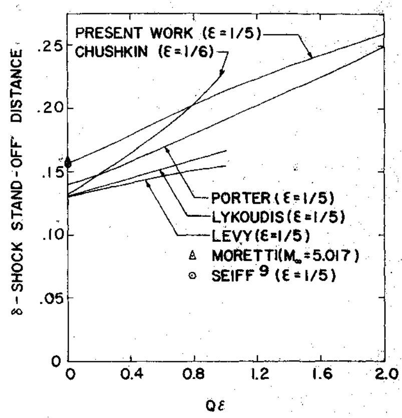

Fig. 3 Shock detachment distance, $\Theta = 0$.

where the bar denotes the arithmetic average of adjacent points in space and the partial derivatives in space in $\mathbf{g}$ are expressed as central differences. The linear stability criteria suggests a limiting time step similar to that of the Courant-Friedrichs-Lewy criteria.[9]

The numerical treatment of boundary points is similar to that of Ref. 10 and is contained in Ref. 11.

Initial values for the computation were obtained by linear interpolation between an assumed stationary shock and a body subjected to inviscid flow behind a normal shock. In varying parameters, the results of previous calculations were employed as initial conditions if they were considered closer to the new steady state.

The results for non-MHD flow were checked with those of a similar method of Moretti[2] and those of the integral method of Belotserkovskii.[13] At moderate supersonic speed, a mesh size of $\Delta\varphi = 0.1$ and $\Delta\Theta = 5°$ was found acceptable. An increase in speed required a finer mesh, perhaps because of the larger gradients in the shock layer.

The subsonic region is increased in extent because of the deceleration effect of the MHD force. The shock shape and sonic line movement are illustrated in Fig. 2. Variable conductivity, $\omega \neq 0$, is not important here because of the fairly uniform temperature of the subsonic region. The centerline detachment distance, Fig. 3, is convenient for comparing theories. The non-MHD value ($Q = 0$) of the present work is substantiated by the similar method of Moretti[2] and the empirical correlation of Seiff[12] [$\delta \doteq (r_s - r_b)/r_b = 0.78\,\epsilon$ where ϵ is normal shock density ratio]. The relative MHD effect is comparible to that obtained by Porter[3,4] (based on Bush[6]), Lykoudis,[5] and Levy et al.[7] The results of Chushkin[8] show a substantially higher MHD effect. This may be due to an increasing error in the integral method of Chushkin as the domain increased without increasing the number of strips employed.

We estimate an approximate doubling of inviscid total drag for $Q\epsilon = 2$. A comparison with experiments[1] requires inclusion of incipient merged viscous effects which is in progress.

References

[1] Kranc, S., Yuen, M. C., and Cambel, A. B., "Experimental Investigation of Magnetoaerodynamic Flow Around Blunt Bodies," CR-1393, Aug. 1969, NASA.

[2] Moretti, G. and Abbett, M., "A Time Dependent Computational Method for Blunt Body Flows," *AIAA Journal*, Vol. 4, No. 12, Dec. 1966, pp. 2136–2141.

[3] Porter, R. W. and Cambel, A. B., "Magnetic Coupling in Flight Magnetoaerodynamics," *AIAA Journal*, Vol. 5, No. 4, April 1967, pp. 803–805.

[4] Porter, R. W. and Cambel, A. B., "Hall Effect in Flight Magnetogasdynamics," *AIAA Journal*, Vol. 5, No. 12, Dec. 1967, pp. 2208–2213.

[5] Lykoudis, P. S., "The Newtonian Approximation in Magnetic Hypersonic Stagnation-Point Flow," *Journal of the Aerospace Sciences*, Vol. 28, No. 7, July 1961, pp. 541–546, 562.

[6] Bush, W. B., "Magnetohydrodynamic-Hypersonic Flow Past a Blunt Body," *Journal of the Aerospace Sciences*, Vol. 25, No. 11, Nov. 1958, pp. 685–690, 728.

[7] Levy, R. H., Gierasch, P. J., and Henderson, D. B., "Hypersonic Magnetohydrodynamics With and Without a Blunt Body," *AIAA Journal*, Vol. 2, No. 12, Dec. 1964, pp. 2091–2099.

[8] Chushkin, P. I., "Magnetized Blunt Bodies in a Hypersonic Gas Flow," *Magnetohydrodynamics*, Vol. 1, No. 1, Jan.-March 1965, pp. 49–55.

[9] Richtmeyer, R. D. and Morton, K. W., *Difference Methods for Initial-Value Problems*, Interscience, New York, 1967.

[10] Masson, B. S., Taylor, T. D., and Foster, R. M., "Application of Godunov's Method to Blunt Body Calculations," *AIAA Journal*, Vol. 7, No. 4, April 1969, pp. 694–698.

[11] Coakley, J. F. and Porter, R. W., "Characteristics at Boundaries in Numerical Gasdynamics," PDL Note 2-69, Nov. 1969, Illinois Inst. of Technology, Chicago, Ill.

[12] Inouye, M., "Shock Stand-off Distance for Equilibrium Flow Around Hemispheres Obtained From Numerical Calculations," *AIAA Journal*, Vol. 3, No. 1, Jan. 1965, pp. 172–173.

[13] Belotserkovskii, O. M., "The Calculation of Flows Past Axisymmetric Bodies With Detached Shock Waves," *Journal of Applied Mathematics and Mechanics*, Vol. 25, No. 3, March 1960, pp. 744–755.

Eddy Viscosity Model for Turbulent Pipe Flow

GDALIA KLEINSTEIN*
New York University, New York

I. Introduction

A UNIFIED viscosity model will be sought here for the entire pipe with the requirement that in order to qualify as an acceptable model it must yield not only a mean velocity distribution, but also a turbulent shear, turbulent energy production rate, and direct viscous dissipation rate, in close agreement with experimental data. This aim, which certainly falls short of the task of explaining the complete structure of turbulence in a pipe, can provide a stronghold on some of the more significant and practical aspects of the mean flow properties.

II. Analysis

1) Overlap region

In his paper, Millikan[1] proposed a derivation of the celebrated log law which was based on a minimum set of a priori assumptions. His derivation proceeded as follows: If in the wall region we accept the law of the wall, $u^+ = f(y^+)$ and in the core region the velocity defect law $u_{\max}{}^+ - u^+ = g(\eta)$, by assuming the existence of an overlap region Σ the only functions f and g which are simultaneously satisfied in Σ are

$$f = u^+ = (1/k_1)\ \ln y^+ + k_2' \tag{1}$$

$$g = u_{\max}{}^+ - u^+ = -(1/k_1)\ \ln\eta + k_2'' \tag{1a}$$

and consistent with these equations the maximum velocity is given by

$$u_{\max}{}^+ = -(1/k_1)\ \ln\delta_\tau + (k_2' + k_2'') \tag{1b}$$

Received August 10, 1970; revision received March 25, 1971. This research was initiated under contract F61052-69-C-0018, Department of the Air Force, European Office of Aerospace Research (OAR), while the author was at Tel-Aviv University, and completed under contract AF-AFOSR-1062-67 at New York University.

* Research Associate Professor of Aeronautics and Astronautics.

In Eq. (1), k_1, k_2', k_2'' are arbitrary constants, $u^+ = u/u_\tau$, $u_{\max}{}^+ = u_{\max}/u_\tau$, $y^+ = yu_\tau/\nu$, $\eta = y/r$, where u_τ is the friction velocity $(\tau_w/\rho)^{1/2}$, r the radius of the pipe and $\delta_\tau = (u_\tau r/\nu)^{-1}$ is the inverse of the Reynolds number based on the friction velocity. Equations (1), (1a) and (1b) may be considered as the limit of the law of the wall, the defect law and the friction law for large Reynolds numbers, or equivalently for small δ_τ.

Introducing the definition of the eddy viscosity in the form $\tau_t = -\langle\rho u'v'\rangle = \rho\epsilon du/dy$ where τ_t is the turbulent shear, into the equation of motion $\tau = \mu du/dy - \langle\rho u'v'\rangle$ yields after nondimensionalization,

$$\tau^+ = \tau/\tau_w = (\tilde\epsilon + \delta_\tau)du^+/d\eta \tag{2}$$

where $\tilde\epsilon = \epsilon/u_\tau r$.

Taking the limit of Eq. (2) as $\delta_\tau \to 0$, granting that ϵ^+ possesses a regular limit, and utilizing the result obtained for $du^+/d\eta$ in Eq. (1a) gives the eddy viscosity at the limit of infinite Reynolds number as

$$\lim_{\delta_\tau \to 0} \tilde\epsilon = \tilde\epsilon_0 = k_1\eta\tau^+ \tag{3}$$

for the overlap region Σ.

A solution of the pipe problem consists of integrating Eq. (2) over the inverval $0 < \eta \leq 1$ at a fixed δ_τ subject to the boundary condition $u^+ = 0$ at $y^+ = 0$. To carry out such an integration the eddy viscosity as obtained in Eq. (3) for the overlap region must be extended in η to cover the interval $0 \leq \eta \leq 1$ and in δ_τ to $\delta_\tau > 0$.

2) Core region

The core region is defined as the region between the overlap region and the center line of the pipe. By its nature the overlap region Σ designates the location where viscous effects subside and turbulent effects become predominant. Thus as the overlap region is traversed in the direction of the core, the flowfield becomes more turbulent than viscous in nature and consequently the interaction between turbulent shear stress and viscous shear stress can be expected to decline further, excluding possibly the immediate vicinity of the center line itself. In the limit of small but non zero δ_τ it is therefore assumed that within the core region the turbulent momentum transport coefficient is the same as the turbulent transport coefficient in the overlap region at $\delta_\tau = 0$ viz.,

$$\tilde\epsilon_c = (\tilde\epsilon)_{\delta_\tau=0} = k,\eta\tau^+ \tag{4}$$

where $\tilde\epsilon_c$ designates $\tilde\epsilon$ in the core region C.

The equation of motion for the core becomes then

$$\tau^+ = (\tilde\epsilon_0 + \delta_\tau)du^+/d\eta \tag{5}$$

which is valid for $0 < \delta_\tau \ll 1$ and $\eta_c < \eta < 1$. Equation (5) states that within the core region the total shear is obtained as a superposition of the turbulent and viscous shear with zero interacting terms. These physical assumptions, once accepted, have the following mathematical implication: Let $\tilde\epsilon(\eta,\delta_\tau)$ have a regular asymptotic expansion in C with respect to δ_τ of the form,

$$\begin{aligned}\tilde\epsilon(\eta,\delta_\tau) &= \tilde\epsilon_0(\eta) + \delta_\epsilon\tilde\epsilon_1(\eta) + \ldots \\ &= \tilde\epsilon_0(\eta) + (\delta_\epsilon/\delta_\tau)\delta_\tau\tilde\epsilon_1(\eta) + \ldots\end{aligned} \tag{6}$$

where δ_ϵ is a small parameter which depends on δ_τ so that $(\delta_\epsilon/\delta_\tau) \to 0$ as $\delta_\tau \to 0$. Substituting Eq. (6) into Eq. (2) yields

$$\tau^+ = [\tilde\epsilon_0(\eta) + (\delta_\epsilon/\delta_\tau)\delta_\tau\tilde\epsilon_1(\eta) + \ldots + \delta_\tau]du^+/d\eta \tag{7}$$

Comparing Eq. (7) and Eq. (5) indicates that the consequence of the assumption made in Eq. (4) is equivalent to assuming $\delta_\epsilon \sim 0(\delta_\tau{}^{1+\alpha})$ where $\alpha > 0$. Carrying the mathematical argument farther, since $\tilde\epsilon$ must depend continuously on δ_τ as η changes from C to Σ one obtains for the overlap region the expansion for nonzero δ_τ in the form,

$$\tilde\epsilon(\eta,\delta_\tau) = \tilde\epsilon_0(\eta) + \delta_\tau{}^{1+\alpha}\tilde\epsilon_1(\eta) + \ldots \tag{8}$$